pH- and Metal Ion-Linked Stability of the Hemopexin−Heme Complex†

Federico I. Rosell, Marcia R. Mauk, and A. Grant Mauk*

Department of Biochemistry and Molecular Biology and Centre for Blood Research, University of British Columbia, Vancouver, British Columbia V6T 1Z3, Canada

Received September 15, 2004; Revised Manuscript Received November 17, 2004

ABSTRACT: Thermal denaturation of the human hemopexin−heme complex was investigated under a variety of solution conditions to identify factors that influence heme release. The midpoint temperature for the transition between the folded and folded states, T_m, of the hemopexin−ferriheme complex exhibits a significant dependence on pH. When the pH is reduced from 7 to 5 (50 mM BisTris buffer and 50 mM NaCl), T_m decreases by ∼23 °C despite the relatively higher chloride concentration that tends to stabilize the protein. The thermal stability of the hemopexin−ferroheme complex was examined at pH 7.4 to yield a T_m that is 3.2 °C lower than that of the hemopexin−ferriheme complex under identical conditions. The effect of transition metal ions, which hemopexin has recently been shown to bind [Mauk, M. R., Rosell, F. I., Lelj-Garolla, B., Moore, G. R., and Mauk, A. G. (2005) *Biochemistry 44*, XXXX−XXXX], was also considered. Cu^{2+} and Zn^{2+} had the greatest effect, reducing T_m for the transition by 4.8 and 6.5 °C, respectively, relative to the value for the protein in the absence of metal ions {T_m = 64.9 °C [10 mM sodium phosphate buffer (pH 7.4)]}. These metal ions also interfered significantly with the recovery of the native state from the unfolded protein when the protein on returning to 20 °C. The current results demonstrate how the conditions within the endosomes of hepatocytes (pH ∼5.0, [Cl^-] ∼ 60 mM) and the potential presence of transition metal ions or heme iron reduction contribute to the membrane receptor-mediated process of heme release from hemopexin.

Hemopexin (EC 3.2.1.35, MW = 58 000) is a plasma glycoprotein that in healthy individuals circulates as the apoprotein and is available to scavenge heme that is released to blood as a result of hemolysis or tissue damage (for recent reviews, see refs *1*−*3*). Binding of heme to apohemopexin in the plasma prevents the deposition of heme in tissues and the resulting oxidative damage that can be catalyzed by heme[1] (*4*). The hemopexin−heme complex that is formed in this process is quickly removed from the circulation by the liver where heme is dissociated from hemopexin, and the apohemopexin is returned to circulation (*5*).

With the determination of the three-dimensional structure of the rabbit hemopexin−heme complex (*6*), the environment provided to heme bound by hemopexin has been defined in detail. While the identification of the histidyl ligands to the heme iron as His213[2] and His266 resolves the long-standing uncertainty regarding the identity of these residues, other features of the heme binding site provide a structural basis for the stability of the interaction between heme and apohemopexin. In particular, the two heme propionate groups appear to stabilize interaction with the apoprotein through extensive hydrogen bond interactions. The heme 6-propionate group forms hydrogen bonds with His272 and a water molecule that in turn forms a hydrogen bond with His223. Similarly, the heme 7-propionate group forms hydrogen bonds with Tyr176 and -197 and Arg174 and -185. All of these well-defined interactions and the less readily defined hydrophobic interactions that must contribute to the stability of the hemopexin−heme complex presumably account for the high affinity of the protein for heme. At the same time, however, these interactions constitute barriers to the efficient release of heme from hemopexin in the hepatocyte once the complex has been removed from the circulation.

Our recent studies characterizing the interaction of metal ions with hemopexin in the presence and absence of bound heme (*7*) raise the additional possibility that the stability of the hemopexin−heme complex may be subject to modulation by exposure to various transition metal ions. To address this possibility and the more general question of the factors that influence the stability of the hemopexin−heme complex, we have examined the influence of a variety of environmental factors and the influence of transition metal ions on the electronic and circular dichroism (CD) spectra of the complex formed by hemopexin and ferro- and ferriheme. The results reveal a dependence of complex stability on a number of factors that may be relevant to the mechanism by which heme is released from hemopexin *in vivo*.

† This work was supported by Canadian Institutes of Health Research Operating Grant MOP-53131 and a Canada Research Chair (A.G.M.). The Canadian Foundation for Innovation provided funds for the spectropolarimeter (through the University of British Columbia Laboratory of Molecular Biophysics) and the spectrophotometers.

* To whom correspondence should be addressed: Department of Biochemistry and Molecular Biology, Life Sciences Centre, 2350 Health Sciences Mall, University of British Columbia, Vancouver, BC V6T 1Z3, Canada. Telephone: (604) 822-3719. Fax: (604) 822-6860. E-mail: mauk@interchange.ubc.ca.

[1] Abbreviations: heme, iron protoheme IX; PBS, phosphate-buffered saline.

[2] All sequence numbers cited here refer to rabbit hemopexin.

10.1021/bi0480077 CCC: $30.25
Published on Web 01/22/2005

EXPERIMENTAL PROCEDURES

Sample Preparation. Human apohemopexin was isolated from blood plasma cryosupernate (Canadian Blood Services) and reconstituted with ferriprotoporphyrin IX as described in detail elsewhere (*7*). After the final purification step involving immobilized nickel affinity chromatography (Hi-Trap Chelating HP, Amersham Biosciences), the holoprotein was incubated in a chelating buffer [20 mM sodium phosphate, 50 mM EDTA, and 500 mM sodium chloride (pH 7.4)] to remove trace metal ions. The protein was then exchanged into stock buffer [10 mM sodium phosphate (pH 7.4)] by repeated centrifugal ultrafiltration (Amicon Ultra, 10 000 NMWL, Millipore). Immediately prior to each experiment, protein samples (0.5 mM hemopexin−ferriheme, $A_{414}/A_{280} = 0.96$ at pH 7.4) were diluted to a final protein concentration of ∼5 μM in a variety of buffers. The effects of selected transition metal ions were examined in a stock buffer containing 100 μM $Zn(NO_3)_2$, $Ni(NO_3)_2$, $MnCl_2$, $CoCl_2$, or $CuCl_2$. These metal ion solutions were prepared from atomic absorption standards (VWR, Merck). The protein stability in the stock buffer was compared to that in PBS [10 mM phosphate buffer, 2.7 mM KCl, and 137 mM NaCl (pH 7.4)] or a phosphate-buffered nitrate solution [10 mM phosphate buffer, 2.7 mM KNO_3, and 137 mM $NaNO_3$ (pH 7.4)] to examine specific electrolyte effects. Finally, the influence of pH on the protein was examined in the range of 5.0−7.0 in 50 mM BisTris buffer containing 50 mM NaCl. For thermal denaturation studies by electronic absorption spectroscopy, each protein sample (0.8 mL) was placed into a masked, semi-micro quartz cuvette (path length of 1 cm) and overlaid with light mineral oil. The cuvette was sealed with DuraSeal. For far-UV circular dichroism measurements, the protein solution (400 μL) was placed into a quartz cuvette (path length of 1 mm) fitted with a Teflon stopper.

Samples of the hemopexin−ferroheme complex were prepared in an anaerobic glovebox by addition of solid sodium dithionite to a concentrated sample of the hemopexin−ferriheme complex. Excess reducing agent was removed by repeated centrifugal ultrafiltration (Microcon YM-30, Millipore) and dilution with fresh, deoxygenated stock buffer. Samples of the hemopexin−ferroheme complex were diluted ∼100 fold with the desired deoxygenated buffer (1.6 mL; final protein concentration of ∼4 μM) in an anaerobic cuvette, and then overlaid with light mineral oil that had been deoxygenated. The cuvette was sealed with a rubber septum before the sample was removed from the glovebox for spectroscopic analysis. These larger sample volumes were stirred during thermal denaturation to ensure a uniform temperature throughout the sample. The CO adduct of the hemopexin−ferroheme complex was prepared by diluting the reduced protein with a solution that was saturated with CO (1 atm; Praxair). For some thermal denaturation experiments, an excess of sodium dithionite was added prior to the cuvettes being sealed with the rubber septa. The amount of dithionite present was never sufficient to contribute significantly to the absorbance spectrum in the Soret region.

Thermal Denaturation Experiments. Thermal denaturation of the hemopexin−ferriheme and hemopexin−ferroheme complexes was carried out under computer control with either a Cary UV−vis spectrophotometer (model 4000 or 6000i) or a Jasco spectropolarimeter (model J-810), each of which was equipped with Pelletier devices. The temperature probes of the three instruments were calibrated with respect to the true temperature of the solution in the cuvette as measured with a Fluke model 2175A digital thermometer fitted with a subminiature copper−constantan thermocouple that was, in turn, calibrated with high-accuracy mercury thermometers. For thermal denaturation monitored by electronic spectroscopy, spectra (260−800 nm) were collected every 2.5 °C after the sample was equilibrated for 1 min at each temperature. Overall, the average temperature gradient was ∼1 °C/min. The same temperature gradient was used to monitor thermal denaturation of the protein by circular dichroism spectroscopy.

Data Analysis. The thermodynamic parameters associated with the temperature-induced denaturation of the hemopexin−heme complex were obtained by nonlinear, least-squares analysis of the temperature dependence of the protein absorption or circular dichroism at selected wavelengths. In these analyses, a two-state denaturation process was assumed when fitting the data to eqs 1 and 2 (*8*) with Scientist (Micromath). A_F and A_U are the absorbances of the folded and unfolded states, respectively, of the protein extrapolated to 0 K, and m_F and m_U are the slopes of the linear temperature variation of these absorbances immediately before and after the melting transition, respectively.

$$\mathrm{Abs}(T) = \frac{(A_F + m_F T) + (A_U + m_U T)\exp\left(\frac{-\Delta G_U}{RT}\right)}{1 + \exp\left(\frac{-\Delta G_U}{RT}\right)} \quad (1)$$

$$\Delta G_u(T) = \Delta H_m\left(1 - \frac{T}{T_m}\right) + \Delta C_p\left[T - T_m - T\ln\left(\frac{T}{T_m}\right)\right] \quad (2)$$

where T is the temperature in kelvin, R the gas constant, T_m the midpoint temperature for the transition, ΔH_m the enthalpy change for the transition, ΔG_u the free energy associated with the transition, and ΔC_p the change in heat capacity for the transition, which is assumed to be temperature-independent. To simplify the comparison of various thermal denaturation experiments, the extent of protein denaturation is presented here as the fraction of unfolded protein as calculated with eq 3 (*9*).

$$\text{fraction unfolded} = \frac{(Tm_f + A_F) - A(T)}{(Tm_f + A_F) - (Tm_u + A_U)} \quad (3)$$

The ability of denatured hemopexin to refold after thermal denaturation was estimated either from the absorbance recovered at the Soret maximum relative to the total absorbance lost at this wavelength or from the ellipticity recovered at 231 nm. These parameters are reported as a percentage, and they were determined both immediately after each test solution was returned to 20 °C and again after 24−48 h. On the basis of prior work (*10*−*15*), the use of the van't Hoff formalism that is implicit in eqs 1 and 2 is valid for the analysis of the temperature-dependent spectroscopic changes exhibited by proteins even in cases where the thermal denaturation is only partially reversible (*vide infra*).

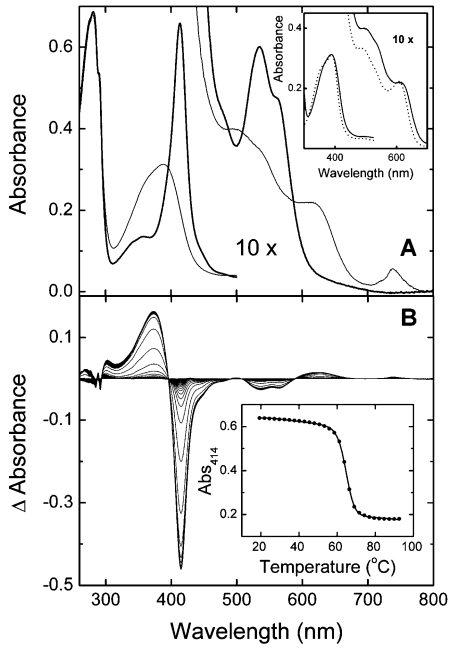

FIGURE 1: Thermal denaturation of the human hemopexin−ferriheme complex in sodium phosphate buffer (10 mM, pH 7.4) monitored by electronic spectroscopy. (A) Comparison of the spectra of the complex collected at 20 (thick line) and 90 °C (thin line). The inset shows spectra of the denatured protein (solid line) and ferriheme at 80 °C (dotted line). The band at 750 nm reflects an increased transmittance across the masked cuvette. (B) Difference spectra obtained by subtracting the spectrum collected at 20 °C from all other spectra. The inset illustrates the temperature dependence of the Soret absorbance; the solid curve represents the nonlinear least-squares fit of these data to eqs 1 and 2.

RESULTS

Spectroscopic Manifestations of Stability of the Hemopexin−Heme Complex. Thermal denaturation of the hemopexin−ferriheme complex is characterized in the UV−vis spectrum by a decreased absorbance at 414 and 530 nm and concomitant increases around 390 and 620 nm (Figure 1A). These spectroscopic changes indicate that the low-spin, bis-His coordination of the heme iron in the native state of the protein is disrupted to produce a high-spin species at elevated temperatures. The spectrum of the unfolded protein resembles that of free heme collected at the same temperature (Figure 1, inset), suggesting that the spin state change is a consequence of heme release by the protein. Ellipticity of this complex around 197 and 230 nm in the far-UV region of the CD spectrum also decreases with an increase in temperature (Figure 2), which reflects a decrease in the level of secondary structure (∼197 nm) and other structural changes that involve the many Trp residues (*16*) and disulfide bonds (*17*) in the protein (∼230 nm). While the role of disulfide bonds in this feature of the UV CD spectrum of hemopexin has not been considered previously, such a contribution is plausible owing to the presence of six disulfide bonds in the structure of this protein (*6*).

Analysis of the temperature dependence of the Soret absorbance (Figure 1B, inset) or other visible absorbance bands with a model for a two-state transition (eqs 1 and 2) yielded a midpoint transition temperature (T_m) of 64.6(3) °C, a van't Hoff enthalpy (ΔH) of 105(5) kcal/mol, and a heat capacity change (ΔC_p) of 3.7(3) kcal mol^{-1} K^{-1} (Table 1). The ΔC_p values calculated from a similar analysis of the

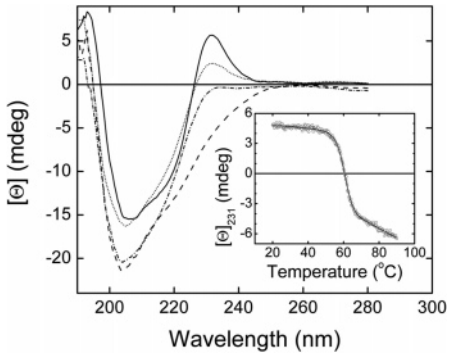

FIGURE 2: Far-UV CD spectra of the human hemopexin−ferriheme complex in 10 mM sodium phosphate buffer (pH 7.4). Spectra were collected prior to heating (—), at 90 °C following a 1 °C/min temperature ramp (- - -), immediately after the sample had been cooled to 20 °C (-·-), and immediately after melting at a rate of 120 °C/min and cooling to 20 °C (···). The inset illustrates the change in ellipticity at 231 nm with temperature during a 1 °C/min ramp. The nonlinear, least-squares fit of these data to eqs 1 and 2 is represented by the solid curve.

protein thermal denaturation monitored by CD spectroscopy at 231 nm were essentially the same, but the T_m and ΔH were lower by 3.8 °C and 14 kcal/mol, respectively, suggesting that changes in the protein fold precede heme release.

As indicated in Table 1, following thermal denaturation with a ramp of 1 °C/min (20−90 °C), ∼35% Soret absorbance of the hemopexin−heme complex was recovered immediately after returning the sample to 20 °C. This recovery increased after prolonged incubation at this temperature. By contrast, recovery of ellipticity at 231 nm following identical treatment of the sample was slightly greater than that observed by electronic spectroscopy and was significantly greater (∼75% recovery) immediately after exposure to the more rapid thermal gradient (120 °C/min; Figure 2) that could be achieved with a thermal cycler. Finally, thermal unfolding of the complex with varying thermal gradients [0.1, 1.0, and 2.5 °C/min; 10 mM sodium phosphate buffer (pH 7.4)] as evaluated by the near coincidence of the pre- and post-transition Soret absorbance values established that variation of this parameter has no significant influence on the extent to which the protein is unfolded.

Transition Metal Ion Linkages of the Stability of the Hemopexin−Heme Complex. The thermal denaturation of the hemopexin−ferriheme complex in the presence of a 20-fold excess of selected transition metal ions (i.e., Co^{2+}, Cu^{2+}, Mn^{2+}, Ni^{2+}, or Zn^{2+}) elicited essentially the same changes in the UV−vis spectrum observed in the absence of metal ions. The effects of these metal ions are compared in Figure 3A, and the corresponding thermodynamic parameters obtained from numerical fits of these data are summarized in Table 1. Except for Mn^{2+}, which did not significantly change the T_m of the hemopexin−ferriheme complex, the transition metal ions investigated here reduced the T_m by 1.5−6.5 °C. The greatest effect was achieved with Cu^{2+} and Zn^{2+}, which lowered the T_m by 4.8 and 6.5 °C, respectively. These metal ions also interfered significantly with the recovery of absorbance at 414 nm even after prolonged incubation of the denatured protein at 20 °C (Table 1). In the case of Cu^{2+}, the van't Hoff enthalpy and ΔC_p associated with unfolding

Table 1: Thermodynamic Parameters[a] of the Thermal Denaturation of the Human Hemopexin−Heme Complex[b] As Monitored by Electronic Spectroscopy and UV Circular Dichroism[c]

sample conditions	T_m (°C)	ΔH (kcal/mol)	ΔC_p (kcal mol^{-1} K^{-1})	recovery (%) $t = 0$	recovery (%) $t > 24$ h
10 mM sodium phosphate buffer at pH 7.4					
hemopexin−ferriheme	64.6	105	3.7	34	79
hemopexin−ferriheme[c]	60.8	91	3.5	53	nd
with 100 μM Co^{2+}	63.1	111	4.1	22	49
with 100 μM Cu^{2+}	59.8	66	2.2	2	0
with 100 μM Mn^{2+}	64.4	107	3.8	32	61
with 100 μM Ni^{2+}	61.0	102	3.8	9	18
with 100 μM Zn^{2+}	58.1	90	3.5	4	8
PBS[d]	72.5	182	5.9	32	61
PBS[d] with Zn^{2+}	70.9	140	4.6	5	10
P_i/NO_3^- [e]	70.7	182	6.1	38	58
P_i/NO_3^- [e] with Zn^{2+}	68.9	152	5.2	6	19
hemopexin−ferroheme	61.4	79	2.7	32	nd
hemopexin−ferroheme−CO	>77	−	−	nd	nd
50 mM BisTris buffer and 50 mM NaCl					
pH 7.0	69.9	158	5.3	38	49
pH 6.5	67.0	158	5.5	39	44
pH 6.0	62.6	147	5.7	33	41
pH 5.5	55.8	120	5.3	26	30
pH 5.5[c]	56.8	121	5.2	34	nd
pH 5.0	46.8	108	3.8	15	nd
pH 5.0 with Zn^{2+}	43.8	106	6.5	nd	nd
pH 5.5/ hemopexin−ferroheme	∼43	−	−	nd	nd
10 mM sodium acetate buffer pH 5.0	44.7	53	1.3	25	nd

[a] On the basis of the reproducibility of the thermodynamic parameters obtained from nonlinear, least-squares regression analysis of replicate thermal denaturation data sets (ΔA_{Soret}), the error in T_m is estimated to be ±0.3 °C. Likewise, the errors associated with ΔH and ΔC_p are estimated to be approximately ±5 kcal/mol and ±0.3 kcal mol^{-1} K^{-1}, respectively. [b] The hemopexin concentration is ∼5 μM for hemopexin−ferriheme samples and 2−4 μM for hemopexin−ferroheme samples. [c] Monitored by CD at 231 nm. [d] In 10 mM phosphate buffer, 2.7 mM KCl, and 137 mM NaCl (pH 7.4). [e] In 10 mM phosphate buffer, 2.7 mM KNO_3, and 137 mM $NaNO_3$ (pH 7.4).

are also substantially lower than those observed for other metal ions.

Electrolyte Linkages of the Stability of the Hemopexin−Heme Complex. Increasing the ionic strength of the hemopexin−ferriheme complex by addition of sodium chloride or sodium nitrate to the buffer stabilized the complex significantly (Figure 3B and Table 1). This result is in agreement with findings of Shipulina et al. that sodium chloride stabilizes rabbit apohemopexin and the rabbit hemopexin−*meso*-heme complex (*14*). In our work, the T_m of the human hemopexin−ferriheme complex increased 6−8 °C in the presence of high concentrations of salt relative to the values observed with samples in phosphate buffer alone, and ΔH and ΔC_p increased 78 and ∼62%, respectively. More interestingly, these salts reduced the destabilizing influence of Zn^{2+} on the complex as demonstrated by a decrease in T_m upon addition of the metal ion that was smaller than that observed at lower ionic strengths. The changes in enthalpy and heat capacity associated with the denaturation of the hemopexin−ferriheme complex in the presence of both Zn^{2+} and a high ionic strength are intermediate between the values obtained in the buffered salt solutions without metal ion and the solution with 100 μM Zn^{2+} in phosphate buffer. Note also that an increased ionic strength did not significantly increase the recovery of the Soret absorbance when the complex was returned to 20 °C despite the stabilizing effect of the high ionic strength on the T_m of the complex. Immediately after thermal denaturation, for example, recovery of this absorbance was comparable to that observed in phosphate buffer alone, but the extent of recovery was not as great after prolonged incubation of the samples at 20 °C. This observation suggests that salts may interfere with the rate of heme rebinding. This effect could be the result of inhibition of electrostatic interactions between important structural elements of the protein at high ionic strengths, or it could result from more extensive adventitious binding of heme to the protein or more extensive formation of heme aggregates.

The hemopexin−ferriheme complex was slightly more stable in PBS than in a phosphate-buffered nitrate solution. The greater increase in T_m induced by chloride could result from favorable interactions of chloride with the protein at sites that are inaccessible to nitrate. As observed in the crystal structure of the rabbit hemopexin−heme complex, a chloride and two sodium ions reside in the central tunnels formed by the propellers of the two domains of the protein (*6*). Consequently, these ions may contribute to the stability of the native form of the complex and account for the lower T_m of the protein observed in 10 mM phosphate buffer.

pH Linkage of Hemopexin−Heme Complex Stability. Electronic spectroscopy of the human hemopexin−ferriheme complex indicates that the complex is stable to dissociation at a pH as low as 5.0 (20 °C). This result is in contrast to the behavior reported for the rabbit hemopexin−ferriheme complex for which 50% of the heme was found to be released at pH 5.0 (*15*). However, thermal denaturation of the human hemopexin−ferriheme complex exhibits a significant dependence on pH (Figure 3C and Table 1). Specifically, the

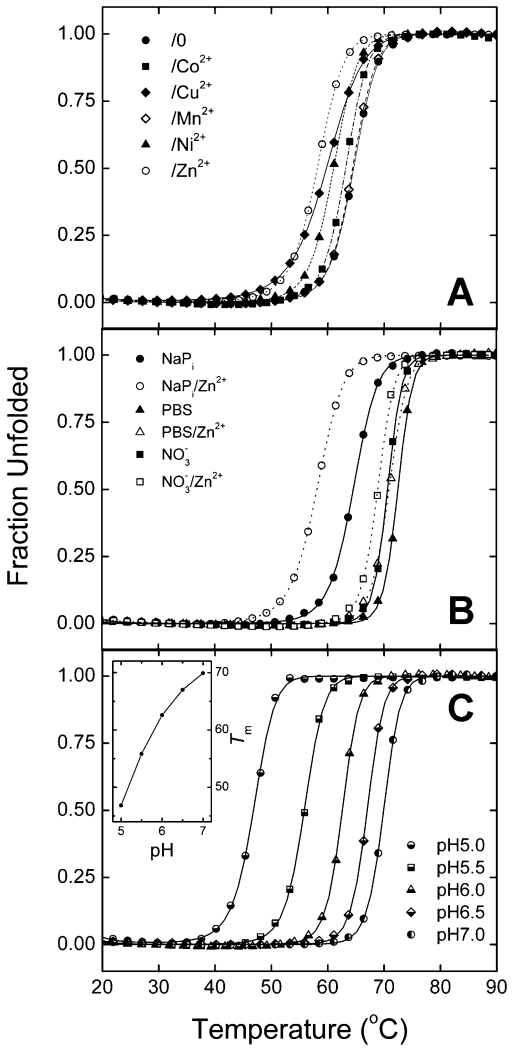

FIGURE 3: Effect of solution conditions on the thermal denaturation of the human hemopexin−ferriheme complex. (A) The effect of metal ions on the thermal denaturation of the protein (●) was examined in sodium phosphate buffer (10 mM, pH 7.4) supplemented with 100 μM $CoCl_2$ (■), $CuCl_2$ (◆), $MnCl_2$ (◇), $Ni(NO_3)_2$ (▲), or $Zn(NO_3)_2$ (○). (B) The influence of added salts on the thermal denaturation of the complex was studied in sodium phosphate buffer (10 mM, pH 7.4) (circles), a phosphate-buffered nitrate solution (squares), or PBS (triangles). Empty symbols and dashed curves denote the inclusion of 100 μM $Zn(NO_3)_2$ in these buffers. (C) The effect of pH on protein stability was determined at pH 5.0 (◒), 5.5 (⬓), 6.0 (half-filled triangle), 6.5 (half-filled diamond), and 7.0 (◐) in BisTris buffer (50 mM) containing NaCl (50 mM). These electronic absorption spectra were analyzed at 414 nm as in Figure 1. For clarity of comparison, the data are presented here as the fraction of protein unfolded, and the curves were generated with the thermodynamic parameters from the nonlinear, least-squares fits of the absorption data to eqs 1 and 2 (Table 1). The inset in panel C shows the pH dependence of the T_m in BisTris buffer (50 mM) containing NaCl (50 mM).

stability of the complex decreases with acidification so that at pH 5.0 the T_m is 23 °C lower than at pH 7.0, and addition of Zn^{2+} (100 μM) reduces T_m an additional 3 °C. Recovery of the Soret absorbance was diminished at lower pH, and the van't Hoff enthalpy decreased by ~32% under such conditions. Replacing the BisTris buffer with sodium acetate (10 mM) at pH 5.0 reduced the T_m by an additional 2 °C (T_m = 44.7 °C), and the changes in enthalpy and heat capacity were dramatically reduced, reflecting a strong influence of buffer on the denaturation of the complex at

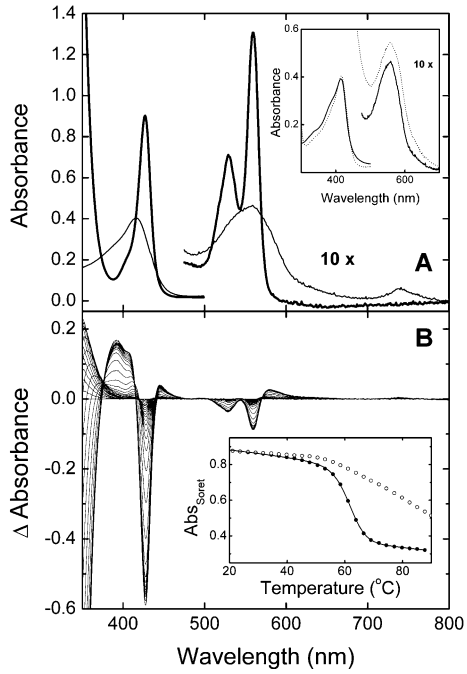

FIGURE 4: Thermal denaturation of the human hemopexin−ferroheme complex in sodium phosphate buffer (10 mM, pH 7.4) in the presence of excess sodium dithionite. (A) Electronic spectra of the human hemopexin−ferroheme complex collected at 15 (thick line) and 90 °C (thin line). The inset shows the spectra of the denatured protein (solid line) and ferroheme (dotted line) measured at 80 °C. (B) Difference electronic spectra obtained by subtracting the spectrum collected at 15 °C from all other spectra to illustrate the thermal denaturation of the hemopexin−ferroheme complex. The inset shows the thermal denaturation profiles of the hemopexin−ferroheme complex (●, Abs_{427}) and the hemopexin−ferroheme complex with CO bound (○. Abs_{421}). The curve represents the nonlinear, least-squares fit to eqs 1 and 2 for denaturation of the complex without CO.

acidic pH. Notably, under these conditions, 13% of the complex is already unfolded at 37 °C, while at higher sodium chloride concentrations, essentially all of the complex remains intact at this temperature.

Oxidation State Linkage of Hemopexin−Heme Complex Stability. The low midpoint potential of the hemopexin−heme complex (*18*) required the addition of an excess of sodium dithionite to ensure that the heme iron remains reduced for the duration of the thermal denaturation experiment even when the samples were prepared in an anaerobic atmosphere, presumably because of the limited integrity of rubber septa under the conditions of our experiment. At pH 7.4 and with an increase in temperature, an absorption maximum developed at 417 nm in the spectrum of the hemopexin−ferroheme complex as the intensity of the Soret band of the complex decreased (Figure 4A). This new feature resembles the Soret band observed in the spectrum of ferrous heme collected at 80 °C and suggests that ferroheme is released from the complex at elevated temperatures. The T_m of the thermal denaturation of the hemopexin−ferroheme complex under these conditions was only 3.2 °C lower than that observed for the complex with ferriheme, while changes in enthalpy and heat capacity were both ~25% lower (Table 1). Spectra collected above 57 °C failed to pass through an isosbestic point on the blue edge of the Soret band, and by 71 °C, the strong absorbance of the excess dithionite began to decrease rapidly as a result of its decomposition, which is facilitated by free heme.

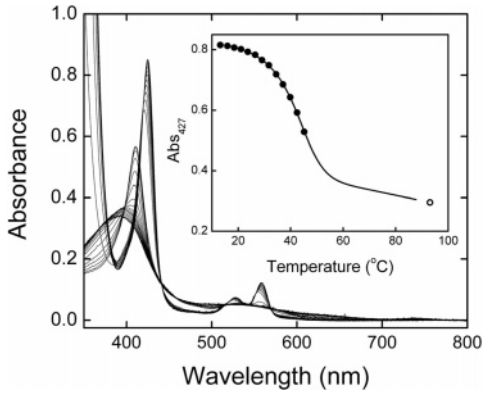

FIGURE 5: Thermal denaturation of the hemopexin−ferroheme complex in BisTris buffer (50 mM) containing NaCl (50 mM) and an excess of sodium dithionite (pH 5.5). The inset shows the partial thermal denaturation profile of the protein monitored at 427 nm. The absorbance at 95 °C (—) was estimated by assuming that at pH 5.5 the extinction coefficients of the folded and denatured protein and m_u are comparable to the corresponding parameters at pH 7.4. The solid curve represents the best fit to eq 1 of the 13 spectra collected prior to the rapid oxidation of the protein at 47.5 °C using these estimates.

In comparison with the hemopexin−ferriheme and −ferroheme complexes, the CO adduct of the hemopexin−ferroheme complex exhibits surprising stability to thermal denaturation at pH 7.4. For this derivative, temperatures well in excess of 100 °C would be required to reach a post-transition baseline. Consequently, thermodynamic parameters for the denaturation of this adduct could not be obtained, but comparison of the thermal stability profiles observed for the CO complex (Soret maximum of 421 nm) and the hemopexin−ferroheme complex (Figure 4B, inset) suggests that the T_m of this complex is greater than 77 °C. Judging from the slopes in the transition region of these plots, it appears that the changes in enthalpy and heat capacity of the CO adduct are also smaller than those of either the hemopexin−ferriheme or −ferroheme complex.

Acquisition of thermal denaturation data for the hemopexin−ferroheme complex at lower pH values proved to be more difficult because of the greater instability and thermal decomposition of dithionite under mildly acidic conditions. In the BisTris/NaCl buffer (pH 5.0 and 20 °C), the hemopexin−ferroheme complex was unstable as reflected by its absorption spectrum, which changed to that of an oxidized species or of a form in which the heme group has been released from the native binding site. For thermal denaturation at pH 5.5 (Figure 5), however, this rapid change from the spectrum of the hemopexin−ferroheme complex coincided with the complete disappearance of the absorbance associated with dithionite just above 45 °C. This observation argues that above 45 °C, the spectrum corresponds to a mixture of the hemopexin−ferriheme complex and free ferriheme. At higher temperatures (>45 °C), the broad band observed at ∼390 nm resembles ferriheme (Figure 1, inset) and is the principal component in the spectrum of the denatured hemopexin−ferriheme complex, consistent with this interpretation. By extrapolation of the change observed at pH 5.5 (at temperatures below those that result in the elimination of the spectroscopic contribution of dithionite) to the total absorbance change observed in the thermal denaturation of the hemopexin−ferroheme complex at pH 7.4, and assuming that the extinction coefficients of the hemopexin−ferroheme complex are independent of pH, we estimate the T_m of the hemopexin−ferroheme complex to be ∼43 °C at pH 5.5 (Figure 5, inset).

DISCUSSION

As discussed above, the hemopexin−heme complex is remarkably stable, yet heme is released from this complex *in vivo* under conditions that permit the liberated apoprotein to return to circulation and continued service (*5*). From the three-dimensional structure of the rabbit hemopexin−heme complex, several hydrogen bonding interactions involving the heme propionate groups have been identified that help stabilize the binding of heme to hemopexin. Dissociation of heme from the complex must, therefore, involve not only protonation of the axial histidyl ligands but also disruption of these hydrogen bonds. Our recent discovery (*7*) that apohemopexin and the hemopexin−heme complex bind metal ions differentially raises the possibility that this new dimension of hemopexin function might also influence the stability of the hemopexin−heme complex. As the stability of the hemopexin−heme complex was likely to be dependent on the binding of metal ions as well as pH, the oxidation state of the heme iron, and specific ion (salt) effects, we have studied the influence of all of these factors together on the stability of the complex formed by the human protein.

The Soret region of the electronic absorption spectrum of the hemopexin−heme complex is a sensitive reporter of the integrity of the complex and can be used to monitor the effect of pH and metal ions on the thermodynamic stability of the complex. While the conventional means of studying the stability of protein secondary structure is to monitor the far-UV CD spectrum, the range of solution conditions required for our study resulted in optical interference that prevented routine use of this approach. However, the hemopexin−heme complex is known to exhibit a positive Cotton effect at ∼230 nm that has been assigned to tryptophanyl residues (*15*, *16*, *19*). A similar Cotton effect has also been suggested to arise from disulfide bonds, possibly interacting with Trp residues (*17*). Thus, monitoring unfolding of hemopexin at this wavelength provides a reasonable alternative means of assessing protein structural integrity. From the combined use of changes in Soret absorbance with changes in the CD spectrum at ∼230 nm or a higher energy, it has been possible to obtain reasonable insight into both the stability of heme binding to apohemopexin and the stability of the protein component of the hemopexin−heme complex.

Under our standard conditions (pH 7.4, 10 mM sodium phosphate buffer), the T_m for the human hemopexin−heme complex as determined from changes in the electronic spectrum observed at 414 nm was ∼4 °C higher than the T_m value determined from the loss in ellipticity at 231 nm, suggesting that some alteration in hemopexin structure occurs during the thermal denaturation immediately prior to heme release. However, at pH 5.5, the T_m values obtained by these methods are nearly coincident with the T_m for heme release, which is 1 °C lower than that for denaturation of the protein. Substantial recovery of the folded state following the thermal denaturation of the ferriheme complex was evident from the return of 230 nm ellipticity. This observation is in contrast to the situation for the rabbit hemopexin−*meso*-heme complex in which this ellipticity was abolished by heating

and not recovered (*14*). Incomplete renaturation of the hemopexin−heme complex presumably reflects to a large extent the fact that this protein is both large and glycosylated. In addition, heme released by thermal unfolding may be partially sequestered as the result of nonspecific binding to the protein or aggregation.

A potential role for metal ions in the modulation of heme binding during the transport and release of heme is substantiated by the finding that metal ions alter the thermodynamics of the dissociation of the heme group from hemopexin. Notably, Cu^{2+} reduces the T_m of the complex, and it also decreases the enthalpy and heat capacity of heme dissociation relative to the situation encountered in the absence of metal ions. The reduced ΔH associated with the denaturation of hemopexin in the presence of Cu^{2+} may result from the occurrence of species intermediate between the folded and unfolded forms of the protein (*13*). This interpretation is consistent with the observation that the isosbestic points obtained in the presence of Cu^{2+} are less well defined than those observed during denaturation in the presence of other metal ions. Such intermediates might arise from altered heme binding geometries or from partial stabilization of normally transient intermediates through binding of Cu^{2+}. Of the five metal ions examined, Zn^{2+} causes the most significant decrease in the T_m of the hemopexin−heme complex. Even at elevated chloride concentrations (which stabilize the complex significantly), Zn^{2+} exhibits a destabilizing influence on the complex, albeit to a lesser degree than in the absence of chloride. These results may indicate that metal ion binding occurs in the vicinity of the heme group, thereby permitting a relatively rapid effect of metal ion binding on the stability of the complex. In fact, the inability of the complex to recover significantly when the sample is cooled following thermal denaturation in the presence of certain metal ions could indicate competition of these metal ions with the heme group for critical protein ligands, perhaps even one of the axial ligands to the heme iron (His213 and -266).

The apparently additive but opposite influence exerted by salts and metal ions on the thermal stability of the hemopexin−heme complex stresses the significance of the overall composition of the solution on the properties of the protein. In hepatic endosomes, for example, the chloride concentration is 50−70 mM (*20*, *21*), a situation that would stabilize the hemopexin−heme complex. However, the pH within these vesicles is also acidic [pH ∼5.0 (*22*−*24*)]. The studies presented here reveal a pronounced destabilization of the hemopexin−heme complex as the pH is lowered such that under conditions approximating those found in endosomes, the human hemopexin−ferriheme complex exhibits a T_m at least 25 °C lower than it exhibits in PBS. This result is in sharp contrast to an earlier report that the thermal stability of the rabbit hemopexin−*meso*-ferriheme complex is essentially independent of pH (*14*). In another important divergence from the results found for the rabbit hemopexin−*meso*-heme complex, we find that the thermal stability of the human hemopexin−heme complex is only weakly dependent on oxidation state at pH 7.4. Nevertheless, the stability of the hemopexin−ferroheme complex is far more dependent on pH than that of the hemopexin−ferriheme complex.

The data analysis we have used assumes a two-state transition (folded ⇌ unfolded) as was the case for the previous study of the rabbit hemopexin−*meso*-heme complex (*14*). Nevertheless, it is difficult to compare directly the results from the two species of protein because of differences in the way the analyses were performed (*14*, *16*). For example, some of the T_m values reported by Shipulina et al. (*14*) simply represent the temperature at which 50% of the total Soret absorbance change was observed without consideration of the temperature-dependent changes in the extinction coefficients of the protein before and after the transition. T_m values determined in this manner (*14*) are influenced by the temperature range that is examined. Consequently, considerable differences can result between the thermodynamic parameters derived by this method and those derived from more comprehensive analysis as employed in the current study and elsewhere (*8*−*10*). Additional differences may also have arisen because of the failure in the earlier study to address adequately the experimental issues involved in maintaining hemopexin in the reduced state, particularly at elevated temperatures and reduced pH, conditions further complicated by the rapid decomposition of sodium dithionite.

The uptake and entrapment of the hemopexin−heme complex by hepatic endosomes, the release of heme from this complex within the endosome, and the return of apohemopexin to the circulation represent a complex series of events that is initiated by interaction of the complex with a membrane receptor (*25*). The studies presented here evaluate parameters that influence the stability of the hemopexin−heme complex *in vivo* or that are likely to do so. Specifically, we find that the stability of the hemopexin−ferriheme complex decreases as the pH is lowered, that the complex is destabilized in a semiquantifiable manner upon reduction of the heme iron, and that the binding of metal ions significantly decreases the stability of the hemopexin−ferriheme complex. While the hepatic endosomal pH is known to be acidic (*23*, *24*), the metal ion content of endosomes is to the best of our knowledge unknown. Our results provide a rationale for evaluating this property of endosomes.

REFERENCES

1. Morgan, W. T., and Smith, A. (2000) Binding and transport of iron-porphyrins by hemopexin, *Adv. Inorg. Chem. 51*, 205−241.
2. Delanghe, J. R., and Langlois, M. R. (2001) Hemopexin: A review of biological aspects and the role in laboratory medicine, *Clin. Chim. Acta 312*, 13−23.
3. Tolosano, E., and Altruda, F. (2002) Hemopexin: Structure, function, and regulation, *DNA Cell Biol. 21*, 297−306.
4. Holt, S., Reeder, B., Wilson, M., Harvey, S., Morrow, J. D., Roberts, L. J., II, and Moore, K. (1999) Increased lipid peroxidation in patients with rhabdomyolysis, *Lancet 353*, 1241.
5. Smith, A., and Hunt, R. C. (1990) Hemopexin joins transferrin as representative members of a distinct class of receptor-mediated endocytic transport systems, *Eur. J. Cell Biol. 53*, 234−245.
6. Paoli, M., Anderson, B. F., Baker, H. M., Morgan, W. T., Smith, A., and Baker, E. N. (1999) Crystal structure of hemopexin reveals a novel high-affinity heme site formed between two β-propeller domains, *Nat. Struct. Biol. 6*, 926−931.
7. Mauk, M. R., Rosell, F. I., Lelj-Garolla, B., Moore, G. R., and Mauk, A. G. (2005) Metal ion binding to human hemopexin, *Biochemistry 44*, 1864−1871.
8. Niranjanakumari, S., Kurz, J. C., and Fierke, C. A. (1998) Expression, purification and characterization of the recombinant ribonuclease P protein component from *Bacillus subtilis*, *Nucleic Acids Res. 26*, 3090−3096.

9. Pace, C. N., and Scholtz, J. M. (1997) in *Protein Structure: A Practical Approach* (Creighton, T. E., Ed.) pp 299−321, IRL Press at Oxford University Press, New York.
10. Fisher, M. T. (1991) Differences in thermal stability between reduced and oxidized cytochrome b_{562} from *Escherichia coli*, *Biochemistry 30*, 10012−10018.
11. Manly, S. P., Matthews, K. S., and Sturtevant, J. M. (1985) Thermal denaturation of the core protein of lac repressor, *Biochemistry 24*, 3842−3846.
12. Edge, V., Allewell, N. M., and Sturtevant, J. M. (1985) High-resolution differential scanning calorimetric analysis of the subunits of *Escherichia coli* aspartate transcarbamoylase, *Biochemistry 24*, 5899−5906.
13. Hu, C. Q., and Sturtevant, J. M. (1987) Thermodynamic study of yeast phosphoglycerate kinase, *Biochemistry 26*, 178−182.
14. Shipulina, N. V., Smith, A., and Morgan, W. T. (2001) Effects of reduction and ligation of heme iron on the thermal stability of heme-hemopexin complexes, *J. Protein Chem. 20*, 145−154.
15. Wu, M. L., and Morgan, W. T. (1994) Conformational analysis of hemopexin by Fourier-transform infrared and circular dichroism spectroscopy, *Proteins 20*, 185−190.
16. Wu, M. L., and Morgan, W. T. (1993) Characterization of hemopexin and its interaction with heme by differential scanning calorimetry and circular dichroism, *Biochemistry 32*, 7216−7222.
17. Hider, R. C., Kupryszewski, G., Rekowski, P., and Lammek, B. (1988) Origin of the positive 225−230 nm circular dichroism band in proteins. Its application to conformational analysis, *Biophys. Chem. 31*, 45−51.
18. Pasternack, R. F., Gibbs, E. J., Mauk, A. G., Reid, L. S., Wong, N. M., Kurokawa, K., Hashim, M., and Müller-Eberhard, U. (1985) Kinetics of hemoprotein reduction and interprotein heme transfer, *Biochemistry 24*, 5443−5448.
19. Morgan, W. T., and Müller-Eberhard, U. (1974) Modification of tryptophan residues of rabbit hemopexin by *N*-bromosuccinimide, *Enzyme 17*, 108−115.
20. Sonawane, N. D., Thiagarajah, J. R., and Verkman, A. S. (2002) Chloride concentration in endosomes measured using a ratioable fluorescent Cl^- indicator: Evidence for chloride accumulation during acidification, *J. Biol. Chem. 277*, 5506−5513.
21. Sonawane, N. D., and Verkman, A. S. (2003) Determinants of $[Cl^-]$ in recycling and late endosomes and Golgi complex measured using fluorescent ligands, *J. Cell Biol. 160*, 1129−1138.
22. Zak, O., and Aisen, P. (2003) Iron release from transferrin, its *C*-lobe, and their complexes with transferrin receptor: Presence of *N*-lobe accelerates release from *C*-lobe at endosomal pH, *Biochemistry 42*, 12330−12334.
23. Tycko, B., and Maxfield, F. R. (1982) Rapid acidification of endocytic vesicles containing α-2-macroglobulin, *Cell 28*, 643−651.
24. van Renswoude, J., Bridges, K. R., Harford, J. B., and Klausner, R. D. (1982) Receptor-mediated endocytosis of transferrin and the uptake of Fe in K562 cells: Identification of a nonlysosomal acidic compartment, *Proc. Natl. Acad. Sci. U.S.A. 79*, 6186−6190.
25. Smith, A. (2000) Links between cell-surface events involving redox-active copper and gene regulation in the hemopexin heme transport system, *Antioxid. Redox Signaling 2*, 157−175.

BI0480077